Numerical Analysis on Transportation Characteristics of a Self-running Sliding Stage Based on Near-field Acoustic Levitation

Yuanyuan Liu[1], Kheirollah Sepahvand[1], Kai Feng[2] and Steffen Marburg[1]

[1] Chair of Vibroacoustics of Vehicles and Machine,Department of Mechanical Engineering, Technical University of Munich, 85748 Garching, Germany

[2] College of Mechanical and Vehicle Engineering, Hunan University, 410082 Changsha, China

E-Mail: yuanyuan.liu@tum.de

Introduction

Clamping, transferring, and precise positioning of silicon chips or components, which are fragile and have sensitive surfaces, are tough issues in the fields of micro-fabrication, semiconductor handling, and nanotechnology [1] [2]. Conventional non-contact transportation system, i.e., air cushion [3] and magnetic system [4] have some drawbacks. Therefore, a novel self-running ultrasonically-levitated sliding stage has been proposed [5]. Comparing with the other transportation systems [6] [7] which required a guide rail, this self-running stage can reduce the profile and miniaturize the sliding table. This study presents a numerical model to describe the non-contact transportation mechanism and to study the influences of exciting parameters on thrusting forces. The force vibration of the frame has simulated to acquire the film thickness distribution under the traveling wave condition. And then, the nonlinear compressible Reynolds equation can be solved by finite difference methods to obtain the pressure distribution. The influences of exciting factors on the sliding stage dynamics performance are also discussed.

Simplified structure model

The configuration of the sliding stage consists of a rectangular frame and two pairs of PZT plates as shown in Fig. 1. Vibrations in the two side PZTs with different initial phases and amplitudes force the frame to deform and produce a traveling wave along the beam. The traveling wave propagates energy from one side to the other side of the stage, which can push the stage to move along the direction opposite the traveling wave. Therefore, precisely controlled movement based on near-field acoustic levitation (NFAL) theory can be realized.

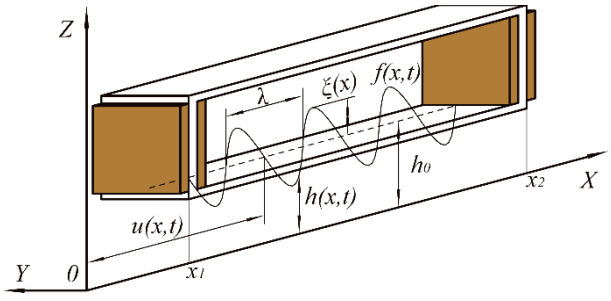

Figure 1: Schematic layout of the self-running sliding stage

In the force vibration analysis, the two pairs of PZT plates working as actuators should be considered in the structure model [Fig. 2]. Owing to its symmetrical structure, only half of the stage is modeled. The vibration equation of the sliding stage can be expressed as

$$[M]\{\ddot{\xi}\}+[K]\{\xi\}=\{F\}, \tag{1}$$

where *[M]*, *[K]*, *{F}* and ξ are the system mass matrix, stiffness matrix, force and vibration deformation.

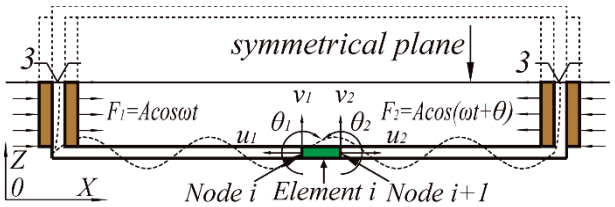

Figure 2: Simplified structure models for force vibration analysis

Governing equations

Reynolds equation

A modified Reynolds equation is solved to obtain the pressure distribution in the air film between the stage and the substrate surface. According to Ref. [8], the Reynolds equation which only considering the *x*-direction movement can be expressed as

$$\begin{aligned}\frac{\partial}{\partial x}\left(ph^3\frac{\partial p}{\partial x}\right)+\frac{\partial}{\partial y}\left(ph^3\frac{\partial p}{\partial y}\right)&=12\mu_0\frac{\partial(ph)}{\partial t}\\&+6\mu_0\dot{u}\frac{\partial(ph)}{\partial x}-\frac{\ddot{u}}{2}\frac{\partial\left(p^2h^3\right)}{\partial x}\end{aligned}, \tag{2}$$

where p, h, μ_0 and u are pressure, film thickness, ambient air viscosity coefficient and sliding stage relative displacement in *x*-direction, respectively.

Dynamics of the stage

Except the sliding stage gravity, two types of external force are applied upon the stage: levitation force and thrust force [9]. The non-uniformity of the pressure gradients in the *x*-direction and the relative movement between the upper and bottom surface of the squeezed film, can develop shear stresses in the film and then produce thrust force acting on the sliding stage. Notably, no trust force is found along the *y*-direction because the mean pressure gradient in the *y*-direction is always zero. For a Newtonian fluid, the total thrust force acting on the stage in the *x*-direction is expressed by [10]

$$F_x = -\int_{x_1}^{x_2}\int_0^D \left(\frac{h}{2}\frac{\partial p}{\partial x} + \mu_0 \frac{\dot{u}}{h} + \frac{\rho h \ddot{u}}{3}\right) dy dx\,, \qquad (3)$$

where D is the width of the stage. The negative sign on the shear stress integration is added because the bottom surface of the plate is normally pointing at the negative z-direction.

The forces acting on the levitated stage in the z-direction includes the gravitational force of the stage, and the supporting force produced by the squeeze film, which is given by

$$F_z = -mg + \int_{x_1}^{x_2}\int_0^D (p - p_a) dy dx\,. \qquad (4)$$

Film thickness-traveling wave condition

When the PZTs at the two sides of the sliding stage are excited by two voltages with different initial phases, they induce two waves with different amplitudes and directions along the beam which, in turn, shall form a combined wave [Fig. 1]. The combined wave expression is given by

$$f(x,t) = \xi_0[a_1 \sin(\omega t - 2\pi\lambda x) + a_2 \sin(\omega t + 2\pi\lambda x)]\,, \qquad (5)$$

where a_1 and a_2 are normalized amplitudes, and λ is wavelength of the combined wave. The combined wave is a mixture of traveling and standing waves.

Thus, the film thickness in the traveling wave condition can be written as

$$h(x,t) = h_0 + \xi_0[a_1 \sin(\omega t - 2\pi\lambda x) + a_2 \sin(\omega t + 2\pi\lambda x)]\,. \qquad (6)$$

Thrusting characteristics results

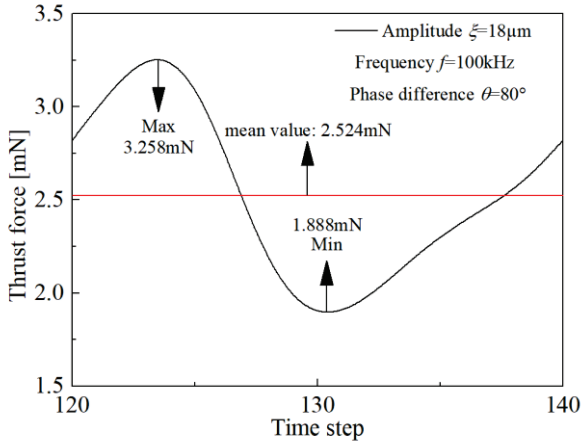

Figure 3: Thrust force within one circle at the driving voltage $80V_{p\text{-}p}$

Figure 3 shows the thrust force within a circle in traveling wave condition. The excitation frequency and the phase difference are f=100 [kHz] and θ=80°, respectively. The length of stage and the driving voltage are 40 [mm] and 80Vp-p, respectively. It is noted that the thrust forces keep positive value in the whole cycle, which means a rightward trust force acts on the sliding stage because of the kinematic viscosity of the air. This trend is consistent with that of a previous investigation [11].

Effect of the driving voltage

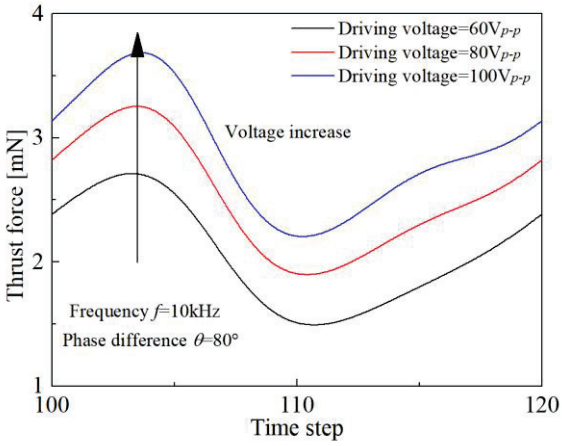

Figure 4: Thrust force versus driving voltage at the same length of stage 40mm

Figure 4 shows the thrust force with increasing driving voltage for the case of f=100 kHz in one excitation cycle at the same θ=80°. It is noted that the peak value of the thrust force increases, indicating that the growth gradient of the thrust force decreases with the increase of driving voltage. In reality, increasing the driving voltage equals to increasing the amplitude.

Effect of the length of stage

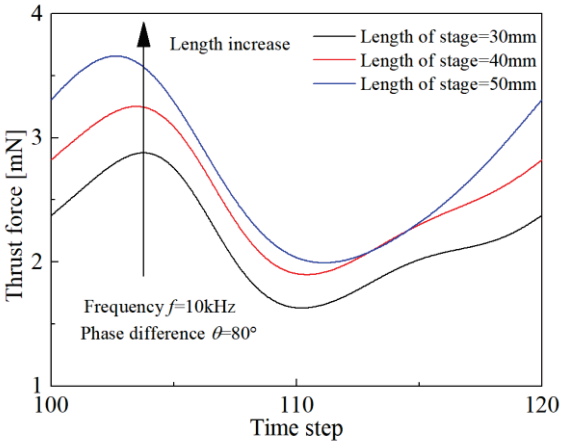

Figure 5: Thrust force versus length of stage at the driving voltage $80V_{p\text{-}p}$

Figure 5 illustrate the thrust force with increasing length of stage in one excitation cycle for the case of f=100 kHz and θ=80°. The results show that the thrust force increases with the increase of the length of stage. However, the growth gradient is very small. This result is due to the fact that longer stage will produce smaller amplitude but have more bigger forced area. Due to the influence of amplitude will be more important, the thrust force will be increases with the

increase of the length of stage [6]. So, the length of stage exists an optimal value.

Conclusions

This paper proposed a simplified structure model of a sliding stage based on the NFAL phenomenon, and presented a numerical analysis of its transportation capacity. The proposed structure model is used to obtain the displacement amplitude distribution using FEM. The Reynolds equation is then solved by FDM to obtain the thrust force. The parametric results show the thrust force increased with the increasing of the driving voltage and the thrust force have a maximum value for an optimal length of stage.

References

[1] Stolarski, T., and Chai, W.: Self-levitating sliding air contact. International Journal of Mechanical Sciences 48(2006), 601-620

[2] Vandaele, V., Lambert P., and Delchambre, A.: Non-contact handling in microassembly: Acoustical levitation. Precision Engineering 29(2005), 491-505

[3] Erzincanli, F., Sharp, J., and Erhal, S.: Design and operational considerations of a non-contact robotic handling system for non-rigid materials. International Journal of Machine Tools & Manufacture 38(1998), 353-361

[4] Kim, O., Lee S., and Han D.: Positioning performance and straightness error compensation of the magnetic levitation stage supported by the linear magnetic bearing. IEEE Transactions on Industrial Electronics 50(2003), 374 - 378

[5] Koyama, D., Nakamura, K., and Ueha, S.: A stator for a self-running, ultrasonically-levitated sliding stage., IEEE Transactions on Ultrasonics, Ferroelectrics, and Frequency Control 54(2007), 2337-2343

[6] Hashimoto, Y., Koike, Y., and Ueha, S.: Transporting objects without contact using flexural traveling waves. Journal of the Acoustical Society of America 103(1998), 3230-3233

[7] Ide, T., Friend, J., Nakamura, K., and Ueha, S.: A non-contact linear bearing and actuator via ultrasonic levitation. Sensors and Actuators A: Physical 135(2007), 740-747

[8] Minikes, A. and Bucher. I.: Noncontacting lateral transportation using gas squeeze film generated by flexural traveling waves--numerical analysis. Journal of the Acoustical Society of America 113(2003), 2464-2473

[9] Koike, Y., Ueha, S., Okonogi, A., Amano, T., and Nakamura, K.: Suspension mechanism in near field acoustic levitation phenomenon. IEEE Ultrasonics Symposium (2000), 671-674

[10] Gross, W., Gas film lubrication. Wiley, 1962

[11] Yin, Y.: Non-contact object transportation using near-field acoustic levitation induced by ultrasonic flexural waves. Ph.D. thesis, 2007